


Review

Imaging Recommendations for Diagnosis, Staging, and Management of Primary Central Nervous System Neoplasms in Adults

Kajari Bhattacharya¹ and Abhishek Mahajan^{2,*} ¹ Tata Memorial Centre, Mumbai 400012, India; kajaribhattacharya7@gmail.com² The Clatterbridge Cancer Centre NHS Foundation Trust, 65 Pembroke Place, Liverpool L7 8YA, UK

* Correspondence: abhishek.mahajan@nhs.net

Simple Summary: Tumors or neoplasms of the central nervous system (CNS) can originate within the CNS (primary CNS neoplasms) or can be secondary to metastases from extra-CNS malignancies. In primary CNS neoplasms, gliomas and meningiomas are the most common groups in adult patients. Gliomas are a diverse group whose prognosis depends upon the histology and increasingly recognized molecular profile of the tumor. Consequently, there have been significant changes in the approach to imaging, management, and follow-up of these patients over the years. Magnetic resonance imaging (MRI) is the primary imaging modality for brain neoplasms, with advanced imaging techniques like perfusion-weighted imaging (PWI) and magnetic resonance spectroscopy (MRS) playing a pivotal role in the post-treatment follow-up setting. With recent advancements in the field of artificial intelligence (AI), we are heading towards a future where AI is bound to become an important player in the diagnosis, management, and follow-up of CNS neoplasms.

Abstract: Central nervous system (CNS) neoplasms are a vast and diverse group of tumors in adults with variable prognoses depending on histology and increasingly understood molecular features. There has been a major paradigm shift in the approach towards these neoplasms ever since the implications of these molecular features have been recognized. Gliomas are the major group of primary CNS neoplasms in adults, and glioblastomas are a significant cause of morbidity and mortality, especially in older patients. Apart from gliomas, meningiomas and pituitary tumors are other major groups. This review aims to elucidate the role of imaging in the screening, diagnosis, management, and follow-up of major primary CNS neoplasms, with an elaborate discussion on the role of artificial intelligence and advanced imaging techniques and future directions likely to play a pivotal role in this ever-evolving subspecialty of oncology.

Keywords: magnetic resonance imaging; glioma; meningioma; perfusion-weighted imaging; magnetic resonance spectroscopy; nuclear imaging; artificial intelligence



Citation: Bhattacharya, K.; Mahajan, A. Imaging Recommendations for Diagnosis, Staging, and Management of Primary Central Nervous System Neoplasms in Adults. *Neuroglia* **2024**, *5*, 370–390. <https://doi.org/10.3390/neuroglia5040025>

Academic Editor: Parisa Gazerani

Received: 12 August 2024

Revised: 6 September 2024

Accepted: 15 September 2024

Published: 1 October 2024



Copyright: © 2024 by the authors. Licensee MDPI, Basel, Switzerland. This article is an open access article distributed under the terms and conditions of the Creative Commons Attribution (CC BY) license (<https://creativecommons.org/licenses/by/4.0/>).

1. Introduction

Central nervous system (CNS) neoplasms are a heterogeneous and diverse group, including benign and malignant tumors, with variable prognoses depending on the histology and molecular features of the neoplasm. The paradigm shift towards considering genetic alterations in CNS tumors, initially incorporated in 2016 and further solidified in WHO CNS-5, is rapidly evolving the imaging and management of these neoplasms, especially gliomas. This review intends to summarize the current imaging recommendations for the diagnosis and management of primary CNS neoplasms.

2. Epidemiology

Primary brain tumors are a heterogeneous group of neoplasms with a wide variation in management and prognosis. These tumors arise from cells within the central nervous

system. A detailed description of the epidemiology of these tumors was given by the Central Brain Tumor Registry (CBTRUS) in 2017, which showed that these neoplasms account for 2% of malignancies. The overall annual incidence rate was 22 per 100,000 population [1].

In India, the incidence of CNS tumors ranges from 5 to 10 per 100,000 population, accounting for 2% of malignancies, similar to the data seen from the CBTRUS. Again, astrocytomas (38.7%) were the most common primary tumors, with the majority being high-grade gliomas (59.5%) [2].

Of the primary CNS neoplasms, around 50% are primary, and the other half are secondary [3]. Meningiomas (18%), glioblastomas (7%), and pituitary tumors (7%) are the most prevalent adult primary CNS neoplasms.

Accordingly, the focus of this review will be on gliomas and meningiomas, with a brief description of imaging recommendations of other entities in relevant sections.

3. Clinical Presentation and Evaluation

As the cranium is a closed cavity, CNS tumors grow at the expense of the normal anatomical contents of the skull or spinal canal. The signs and symptoms vary according to the location and growth rate of the tumors. The presentation can vary from generalized features of raised intracranial tension with headache, nausea, vomiting, papilledema, and altered sensorium to localized symptoms when close to or involving a functional area of the brain, presenting with focal neurological deficits and seizures [4].

In contrast to neoplasms affecting other systems, where non-imaging workup, including tumor markers, plays an important role, the diagnosis and management of CNS neoplasms are primarily dependent on imaging. Thus, cross-sectional imaging is the first method of evaluation of these tumors.

4. Imaging Techniques for CNS Neoplasms

4.1. Computed Tomography (CT)

Contrast-enhanced CT is often the first imaging method used in patients presenting with features of raised intracranial pressure or focal signs, often in cases of acute presentation, to rule out other causes, especially stroke, due to the widespread availability of this modality and the capability of fast imaging. CT-guided stereotactic biopsy is a safe and widely used technique for brain tumor assessment with good diagnostic yield [5]. However, MRI is the imaging modality of choice for the diagnosis and pre-treatment evaluation of brain tumors. CT can be used to evaluate primary osseous tumors of the spine but has a limited role in intradural or intramedullary lesions, and MRI is again the modality of choice [6].

4.2. Magnetic Resonance Imaging (MRI)

MRI plays a major role in the diagnosis, grading, treatment, and response assessment of brain tumors and other intracranial lesions, as described in detail in subsequent sections. Sequences and acquisition parameters for imaging suspected primary intracranial neoplasms need to be modified according to the tumor in question as seen on basic sequences or the clinical scenario (i.e., pre-treatment, post-operative, or follow-up imaging). However, the standard sequences include Axial T2, Axial T1, FLAIR, Coronal T2, Axial GRE/SWI, PWI (preferably T2*), post-contrast Axial T1/FSPGR, post-contrast FLAIR (for leptomeningeal dissemination), and MR spectroscopy (single vs. multivoxel) [7].

Multiparametric MRI, including advanced sequences like diffusion-based sequences, perfusion imaging, MR spectroscopy (MRS), and BOLD imaging (including SWI and functional MRI), plays an important role in the diagnosis, management, and follow-up of CNS neoplasms, as described in Table 1 [8–21].

Table 1. Role of advanced MRI sequences in evaluating CNS neoplasms [8–21].

Purpose		Importance of Sequences
Diagnosis	Benign versus malignant	<ul style="list-style-type: none"> • Diffusion-weighted imaging has a sensitivity of 77% and a specificity of 75%. • Perfusion-weighted imaging has a sensitivity of 91% and a specificity of 88%; • Magnetic resonance spectroscopy has a sensitivity of 77% and a specificity of 63%. • The combination of either DWI and MRS, PWI and MRS, or DWI + MRS + PWI revealed 100% sensitivity and 100% specificity.
	Prediction of histopathology and grading	<ul style="list-style-type: none"> • AUC of 95th percentiles of rCBV was 0.79 (95% CI, 0.67–0.91), and Ktrans was 0.74 (95% CI, 0.59–0.88) for high-grade gliomas. • The rCBV and K-trans of IDH-wildtype glioblastomas are significantly different from IDH-mutant astrocytomas, with a <i>p</i>-value of 0.04 for rCBV and 0.01 for Ktrans. Ktrans showed the highest accuracy for IDH status prediction with an AUC of 0.73 (95% CI 0.57–0.89). • SWI: Higher intratumoral susceptibility signal (ITSS) predicts higher grades in diffuse gliomas. IDH-1 mutation and MGMT promoter methylation were also found to be associated with lower ITSS.
Management	Targeting site of biopsy	<ul style="list-style-type: none"> • Higher-grade parts of the tumor will have high rCBV (PWI) and ITSS (SWI)—which guide the targetable areas.
	Directing path of surgery	<ul style="list-style-type: none"> • DTI: pre-operative planning using DTI gives better yield, shortens operation times, and decreases post-operative neuro-deficits. • Re-evaluation of pre-operative DTI intraoperatively assists in a better visualization of White matter tract shifts, which can be better evaluated at surgery by correlating with pre-operative DTI. • DTI can help decide the initial surgical approach and yield greater GTR rates. • fMRI is a pre-surgical, non-invasive pre-surgical tool to assess the localization of motor and language functions and lateralization of language functions.
Post-treatment evaluation	Response assessment	<ul style="list-style-type: none"> • DWI: Tumor recurrence shows lower ADC values, with reported pooled sensitivity of 71% and specificity of 87% in a recent meta-analysis for differentiating glioma recurrence from radiation necrosis. • MRS: For differentiating recurrent glioma from radiation necrosis, the pooled sensitivity of Cho/NAA was 88% and Cho:Cr was 83%, with the pooled specificity being 86% and 83%, respectively, as shown in a meta-analysis by Zhang et al. [18]. • Pseudoresponse seen with the use of antiangiogenic agents leads to a reduction in vasogenic edema and enhancement with persistently low ADC values, as well as persistent elevation of rCBV. • In pseudoresponse, an expanding area of diffusion restriction corresponds to coagulative necrosis with adjacent viable tumors, and these tumors tend to have a poorer overall prognosis.

Index of abbreviations used: DWI: diffusion-weighted imaging, MRS: magnetic resonance spectroscopy, PWI: perfusion-weighted imaging, AUC: area under the curve, CI: confidence interval, rCBV: relative cerebral blood volume, Ktrans: transfer constant, IDH: isocitrate dehydrogenase, SWI: susceptibility-weighted imaging, ITSS: intratumor susceptibility signal, DTI: diffusion tensor imaging, GTR: gross total resection, fMRI: functional MRI, ADC: apparent diffusion coefficient, Cho: Choline, NAA: N-Acetyl Aspartate, Cr: Creatinine.

4.3. Spinal Imaging

MRI is the modality of choice for imaging the spine [22]. Identifying the epicenter of the tumor as extradural, intradural extramedullary, and intramedullary helps to narrow down the differentials. The basic sequences for spinal tumor imaging are sagittal T1-, T2-, and post-gadolinium T1-weighted sequences, with axial T2- and post-gadolinium T1-weighted images through the lesion [23]. Gradient Recalled Echo (GRE) sequence demonstrates the hemosiderin component of the tumor and exquisitely demonstrates the involvement of vertebral appendages [24]. Diffusion-weighted imaging (DWI) can help differentiate malignant lesions from benign and non-neoplastic etiologies based on lower ADC values in the former [25]. Diffusion Tensor Imaging (DTI) has been used to differentiate ependymomas from astrocytomas based on fiber displacement versus fiber infiltration. Increased FA is seen in more solid tumors [26]. DTI can also aid in surgical planning by demonstrating the relationship of tracts with the tumor. High-resolution 3D-CISS or FIESTA-C sequences acquired in the sagittal or axial plane are utilized for demonstrating the subarachnoid space and lesions better by eliminating CSF flow-related artifacts [27]. The Short Tau Inversion Recovery (STIR) sequence shows marrow abnormalities better and is especially important in imaging of spinal metastases.

4.4. Ultrasonography (USG)

Intraoperative USG has become an increasingly valuable tool in glioma surgery. It offers several advantages for maximizing tumor resection and improving patient outcomes. It provides real-time imaging and helps in tumor localization and mapping, monitoring the extent of resection and, in turn, decreasing intraoperative complications and improving survival and outcomes [28,29].

4.5. Nuclear Medicine

The role of Single-Photon Emission Computed Tomography (SPECT) and Positron Emission Tomography (PET) has significantly evolved in brain tumor imaging over the years. This is described in detail in further sections.

5. Role of Imaging in Primary CNS Neoplasms

5.1. Screening

Screening for primary CNS neoplasms has no survival benefit in the general population and is advised against in the average-risk population [30]. Screening may, however, play an important role in high-risk groups like NF-1. A retrospective review has shown that MRI-based screening of optic pathway glioma may help prevent loss of vision [31]; however, this study included children ages 1–9 years in NF-1. Li-Fraumeni syndrome, associated with the TP-53 mutation, is linked to a multitude of non-CNS and CNS neoplasms, including high-grade diffuse gliomas and choroid plexus carcinomas. Whole-body MRI surveillance, including brain MRI, has been shown to be beneficial [32] and is advised as per NCCN guidelines [33].

Screening of the spine is recommended in medulloblastomas, ependymomas, germ cell tumors, and primary CNS lymphomas in adults [34].

5.2. Diagnosis

Contrast-enhanced MRI forms the cornerstone of imaging in the diagnosis of brain tumors [35]. The routine sequences needed for brain tumor imaging include T1, T2, fluid-attenuated inversion recovery (FLAIR), diffusion-weighted imaging (DWI), and susceptibility-weighted imaging (SWI) or gradient echo imaging (GRE) with a T1-weighted post-contrast sequence (T1 + C). Three-dimensional T1-weighted images like FSPGR (ultra-fast spoiled gradient echo) help in delineating tiny lesions that may be missed on routine sequences with thicker slices. Advanced MRI sequences like perfusion-weighted imaging (PWI), which shows perfusion dynamics of the tumor, and magnetic resonance spectroscopy

(MRS), which shows the metabolite distribution in the tumor, aid not only in diagnosis but help target the most suspicious area for stereotactic biopsy [36].

The role of MRI in pre-treatment imaging of brain tumors is summarized in Table 2 [37].

Table 2. Role of MRI in pre-treatment imaging of CNS tumors.

Localization	Number	Single/Multiple
	Compartment	Intra-axial/extra-axial
		Supratentorial/Infratentorial
	Lateralization	Midline-parenchymal/ventricular
		Lateralized-white matter/grey matter
	Complications needing emergent management	Eloquent/non-eloquent area of the brain significant midline shift, acute obstructive hydrocephalus, trans-tentorial herniation, and brainstem compression
Sequences used		Clinical Utility
	T1	Evaluation of anatomy <ul style="list-style-type: none"> Hyperintensity in precontrast imaging seen in blood products, mineralization, fat, and melanin
Characterization	T2/FLAIR	Evaluation of pathology <ul style="list-style-type: none"> Hyperintensity seen in peritumoral edema (vasogenic and infiltrative), Non-enhancing part of the tumor also appears hyperintense in T2 and may not be differentiable from perilesional edema in glioma. White matter injury due to post-treatment changes and gliosis: Also appears hyperintense but shows volume loss. Intermediate signal intensity: High cellularity, proteinaceous content Low intensity: Bleeding, calcification
	T2*/SWI	<ul style="list-style-type: none"> Pre-treatment gliomas showing bleed having bleed can be considered a higher grade. Bleeds and calcifications can further help in the characterization of some typical lesions. Post-treatment setting: For radiation necrosis, microhemorrhages in radiation-induced vasculopathy. Intratumor susceptibility signal (ITSS): positive correlation with high-grade gliomas
	DWI	<ul style="list-style-type: none"> Diffusion restriction (high signal in DWI and low signal in ADC) is seen in regions of the tumor with increased cellularity and in cytotoxic edema or post-operative injury.
	Post-contrast T1	Postcontrast enhancement reflects the breakdown of the blood–brain barrier.
	MR spectroscopy	<ul style="list-style-type: none"> Higher-grade glioma shows higher Cho/NAA and Cho/Cr ratios than lower-grade glioma with a typical cut-off of Cho: NAA ~2.2 used to characterize high-grade versus low-grade gliomas. Lipid peak represents necrosis in glioma and is seen in lymphomas also, whereas the lactate peak represents hypoxia, respectively. <p>Specific tumor peaks that are seen in some tumors include: Myoinositol: Low-grade diffuse gliomas, Ependymomas Taurine: Medulloblastoma Alanine: Meningioma</p>

Table 2. Cont.

Localization	Number	Single/Multiple	
Pre-surgical planning	PWI	<p>Dynamic Susceptibility Contrast (DSC)—The main metric for tumor evaluation is relative cerebral blood volume (rCBV), the most commonly used technique.</p> <ul style="list-style-type: none"> Higher rCBV is seen in higher grade or progressive/recurrent tumors—Higher grade vs. low grade is typically differentiated with an rCBV cut-off of 1.7. <p>Dynamic Contrast Enhanced (DCE)—Permeability is the main metric for tumor evaluation, denoted by the volume transfer constant (K-trans).</p> <ul style="list-style-type: none"> High permeability is seen in higher-grade or progressive/recurrent tumors. <p>Still predominantly research tool</p> <p>Arterial Spin Labelling (ASL)—the main metric is cerebral blood flow (CBF).</p> <ul style="list-style-type: none"> Noncontrast technique—less commonly used for tumor evaluation. It can be used in pediatric patients and those with contrast allergy. Higher blood flow can be used for tumor grading or to identify progressive/recurrent tumors. 	
		DTI	<ul style="list-style-type: none"> Tractography shows displacement or infiltration of white matter fiber tracts for surgical planning.
		fMRI	<ul style="list-style-type: none"> Task-based fMRI is used for pre-operative functional localization.
		Special sequences	MRA and MRV
	3D-FIESTA/CISS	<ul style="list-style-type: none"> Important in the assessment of extra-axial lesions to assess the relationship with adjacent vessels or nerves Intraventricular obstructive lesions can be better outlined. 	

Figures 1 and 2 show the pre-operative diagnostic and planning MRI in a case of glioma.

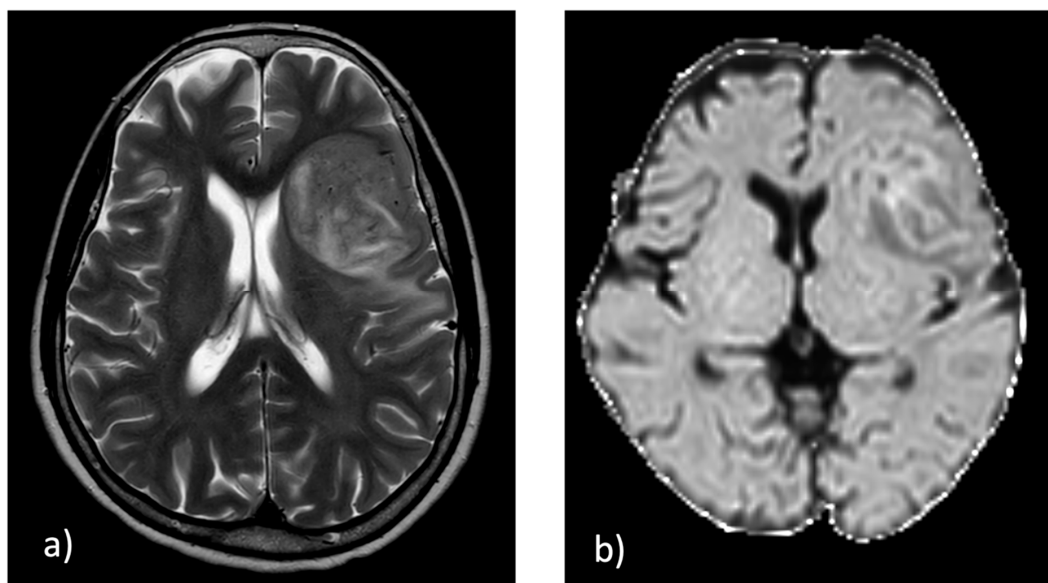


Figure 1. Cont.

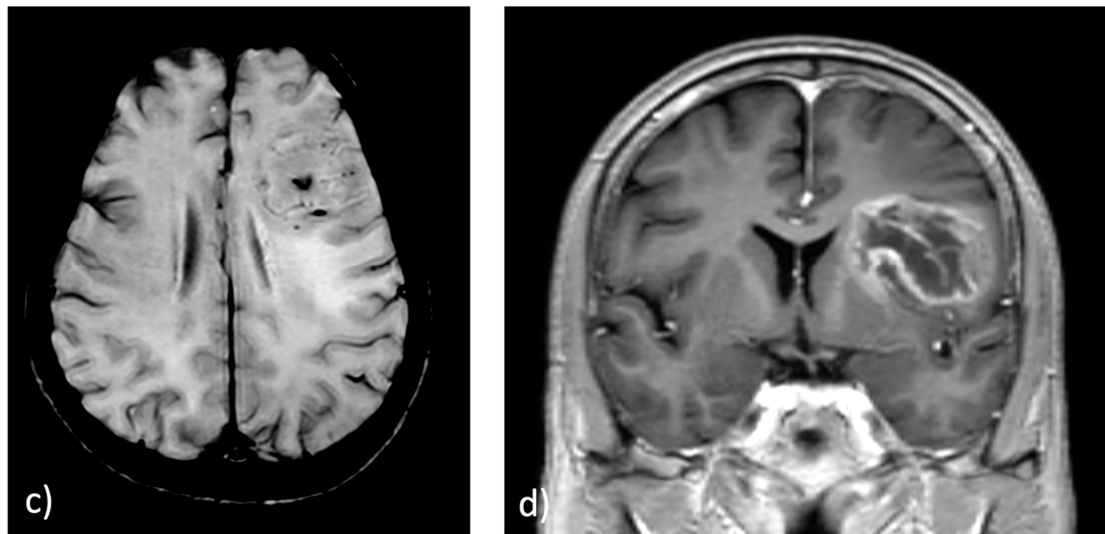


Figure 1. MRI brain—conventional sequences in a 45-year-old female who presents with slurring of speech and left-sided weakness. (a) Axial T2WI shows an isointense to hyperintense signal intensity lesion involving the left fronto-insular region, showing (b) patchy diffusion restriction in axial DWI and (c) Foci of Intratumor Susceptibility (ITSS) in SWI. (d) Coronal post-contrast T1 image shows heterogenous post-contrast enhancement with areas of central necrosis. Imaging features suggestive of high-grade diffuse glioma.

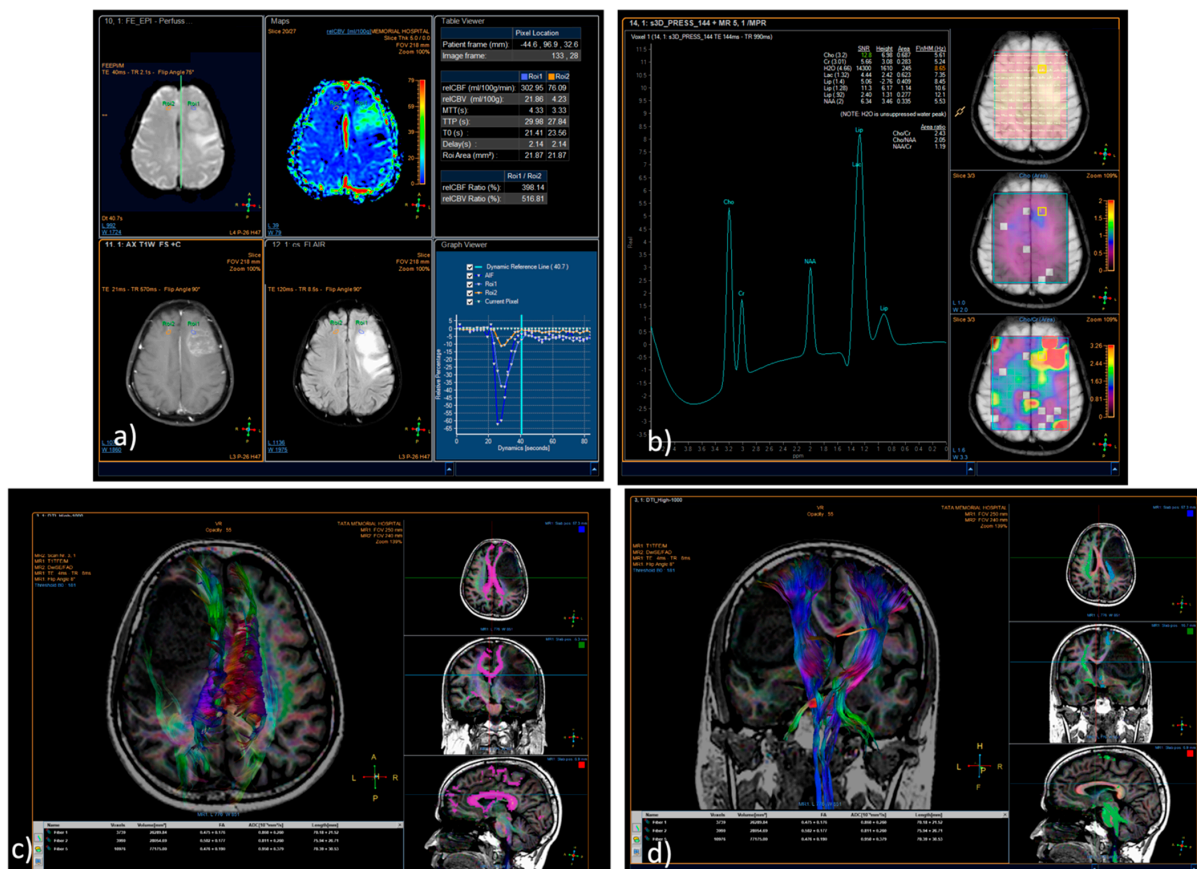


Figure 2. MRI brain—advanced sequences of the same patient as in Figure 1. (a) T2*/DSC-PWI shows elevated rCBV ~7 times in the tumor as compared with NAWM. (b) MRS shows an elevated Choline and decreased NAA, with Cho: NAA = 2.05 and Cho: Cr = 2.43. (c,d) DTI shows the proximity of the tumor to the speech association areas and corticospinal tract.

Figure 3 (flow chart) demonstrates the imaging approach to diagnosis of a suspected CNS primary tumor [38].

Once the imaging diagnosis of a CNS neoplasm is established, further management includes general measures and definitive management.

General measures of management, including management of airway, breathing, and circulation with control of seizures and peritumoral edema by giving steroids, should start before definitive management. Guidelines for the management of major primary CNS neoplasms are summarized in Table 3 [36–50].

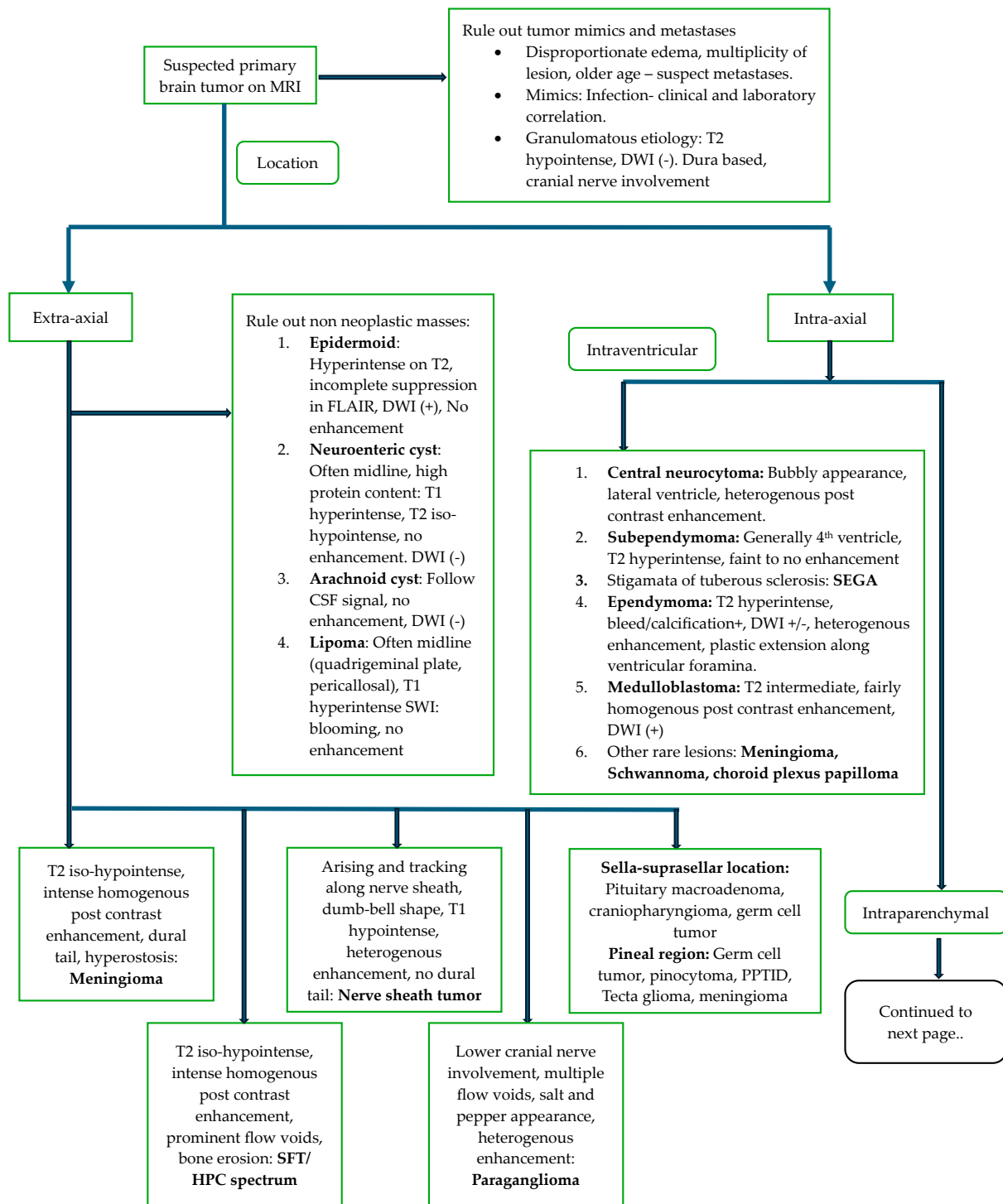


Figure 3. Cont.

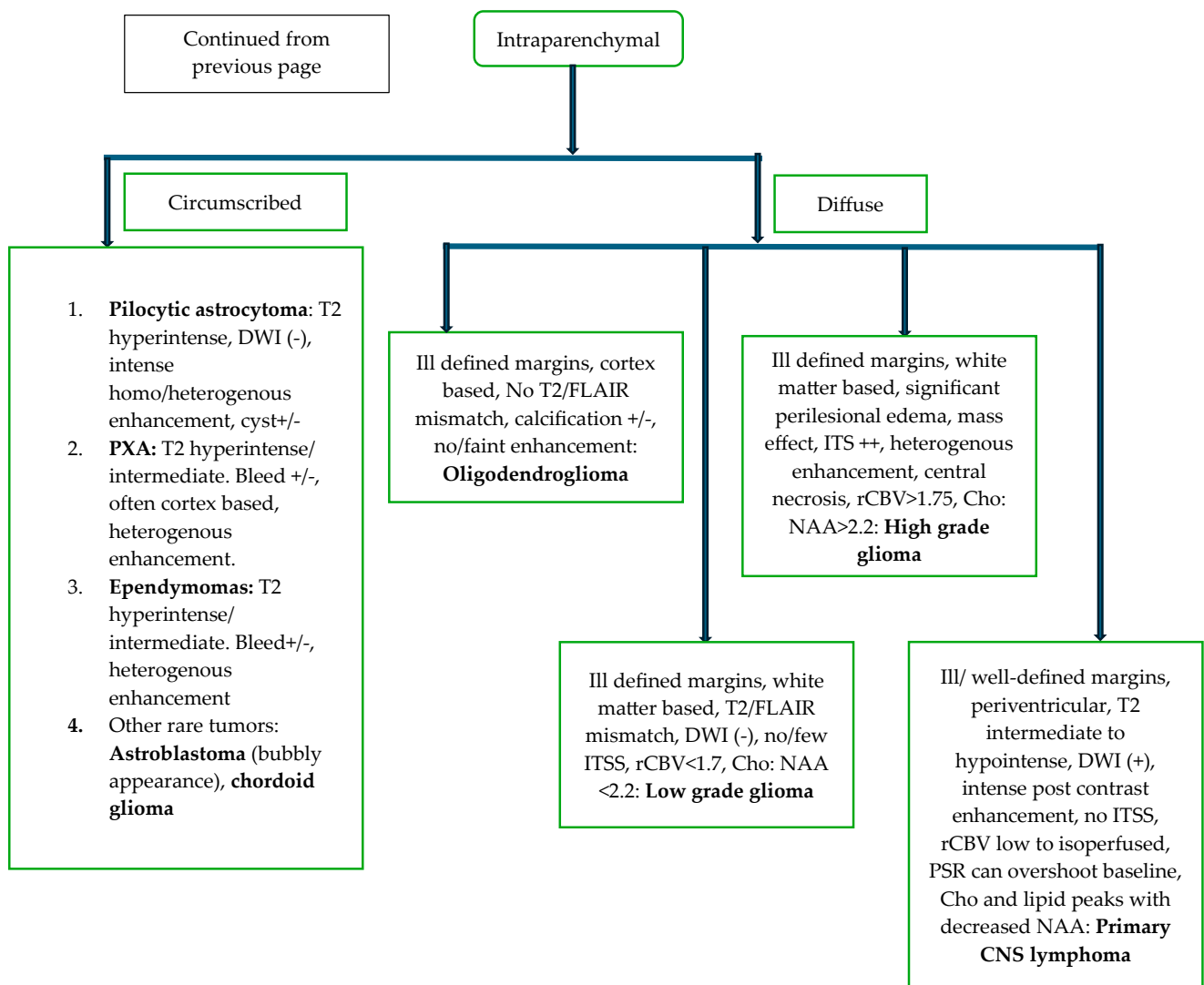


Figure 3. Flow chart demonstrating imaging approach for diagnosis of primary brain tumor in adults.

Table 3. Guidelines for the management of major primary CNS neoplasms in adults.

Tumor	Management
Diffusely infiltrating glioma	<ul style="list-style-type: none"> Maximum possible safe resection is the treatment of choice, followed by radiotherapy and chemotherapy. Stereotactic biopsy: If resection is not feasible due to the eloquence of the involved area IDH-mutant astrocytoma: Maximum possible resection, followed by radiotherapy and chemotherapy depending upon grade. In grade 2 lesions, a PCV (lomustine, procarbazine, and vincristine) regimen is used for subtotal resection and/or when the patient is over 40 years old. In grade 3 and grade 4 patients, radiotherapy and chemotherapy with temozolomide are used. IDH mutant, 1p/19 q-codeleted oligodendroglioma: Maximum possible resection. Radiotherapy, followed by chemotherapy with the PCV regimen if further treatment is needed. Glioblastoma: <70 years of age: maximum possible resection, followed by concomitant radiotherapy and chemotherapy with temozolomide <p>O6-methylguanine-DNA-methyl-transferase (MGMT) methylation status determines the management of elderly who are not candidates for combined radio-chemotherapy.</p>

Table 3. Cont.

Tumor	Management
Meningioma	<ul style="list-style-type: none"> • Symptomatic meningioma—Simpson’s grade 1 resection is indicated. • Conservative management in incidentally detected and asymptomatic lesions. • Lower-grade meningiomas with subtotal resection can be offered radiotherapy or follow-up, whereas higher-grade meningiomas or Simpsons grade 4 or 5/subtotal resections should be given adjuvant radiation. • Incidentally detected meningiomas can be followed up with imaging. • Radiosurgery may be offered in patients with small tumors without mass effect or if surgery is contraindicated.
Pituitary adenoma	<ul style="list-style-type: none"> • Dopamine agonists are used for the management of prolactinomas. • In cases of enlarging non-functioning adenomas that become symptomatic or for functional adenomas, resection is recommended. • Radiation therapy as an adjuvant can be used for residual lesions. • Close follow-up for growing lesions—resurgery may be considered if there is significant growth.

5.3. Intraoperative Imaging

Intraoperative ultrasound has emerged as an important technique for image-guided stereotactic frame-based brain biopsy for tissue sampling in gliomas [47]. It provides real-time imaging for guiding navigation when targeting solid regions of tumors, demonstrating vascularity and contrast enhancement by techniques such as fusion ultrasound [48]. Elastography has shown a promising role in defining tumor margins and parenchymal infiltration, apart from tumor consistency, permitting differentiation of high-grade and low-grade lesions. Intraoperative US has been proposed to be even better than MRI for delineating and guiding the resection of non-enhancing gliomas [49]. Intraoperative MRI has long been in practice but is limited to specialized centers that have the equipment, and it is expensive to operate. It is quasi-real time; hence, it provides near real-time imaging but may not be as immediate as ultrasound during surgery. Hu et al. have demonstrated that combining ultrasound with MRI (USG-MRI fusion) along with contrast-enhanced ultrasound can enhance the extent of resection [51]. This fusion technique allows surgeons to leverage the real-time advantages of ultrasound while benefiting from the pre-operative planning and detailed imaging of MRI.

5.4. Immediate Post-Operative Imaging

Imaging of CNS tumors in the post-treatment setting is of utmost importance and often challenging. Maximal safe resection followed by external beam radiotherapy and chemotherapy remains the standard of care for high-grade gliomas [52,53]. The first or baseline post-operative imaging needs to be performed within 24–48 h of surgery [54,55], as a delay beyond 72 h may lead to confounding effects of subacute hemorrhage/ischemia or reactive post-surgical enhancement, confusing it with residual tumor. For meningiomas, in achievable cases, total resection is attempted as it is associated with lower local recurrence and longer overall survival [56]. Evaluation of residual meningioma is conducted on contrast-enhanced MRI performed within 24–72 h after surgery.

5.5. Follow Up Imaging

The imaging dilemmas and criteria vary with the histopathology of the primary neoplasm in question. Guidelines for management and follow-up imaging are as follows:

5.5.1. Glioma

Maximal safe resection is followed by radiation and chemotherapy in high-risk diffuse gliomas. After completing therapy, the frequency of follow-up intervals should be tailored based on the extent of residual disease, histological features, and genetic tumor

characteristics. IDH-wild-type gliomas typically require shorter imaging intervals, ranging from 2 to 6 months, with more frequent monitoring recommended for higher-risk scenarios. In cases of suspected disease progression, intervals as short as 4 to 8 weeks may be necessary to confirm progression [43]. Radiation induces oxidative stress and inflammation, adversely affecting the vascular endothelium, tumor bed, and normal parenchyma within the radiation field. The side effects of radiation are dose- and time-dependent and can be divided into acute, subacute, or late-delayed effects [57–61]. Pseudoprogression manifests typically within 3–6 months following the start of adjuvant chemoradiation, where initial follow-up imaging may suggest tumor progression, only to later reveal improvement without any change in treatment. In contrast, radiation necrosis tends to occur beyond 6 months after completing therapy, though it can present early, mid-term, or even years later following adjuvant treatment completion. The imaging features of these entities overlap, with punctate T2 hyperintensity with a ‘soap-bubble’ or ‘swiss-cheese’ pattern of enhancement, with no significant diffusion restriction, lipid lactate peaks in MR spectroscopy, and low rCBV [14,15,18,50,62–64] favoring pseudoprogression and radiation necrosis over true progression. Figure 4 illustrates imaging characteristics associated with radiation necrosis. Pseudoresponse refers to the rapid decrease in tumor enhancement and surrounding vasogenic edema following the administration of an antiangiogenic agent, which does not reflect a true anti-tumor response typically observed with Bevacizumab treatment. This phenomenon is likely due to decreased mass effect and vasogenic edema. Typical features of pseudoresponse on post-treatment scans compared to pre-treatment scans include reduced vasogenic edema, decreased enhancement with persistently low ADC values, continued presence of tumor trace, and sustained elevation of rCBV [65,66] (Figure 5).

Radiographic response assessment criteria most widely used for gliomas are described in Table 4 [67–72].

Table 4. Guidelines for post-treatment imaging of glioma.

Criteria	Comment
MacDonald criteria (1990) [67]	<ul style="list-style-type: none"> Based on the largest cross-sectional diameter of contrast-enhancing tumors to assess tumor response. The response is classified into four groups—complete response (CR), partial response (PR), stable disease (SD), and progressive disease (PD). Responses according to these criteria need to be stable for >1 month. Largely replaced by RANO criteria.
RANO criteria (2010) [68]	<ul style="list-style-type: none"> Proposed by the response assessment in the neuro-oncology (RANO) group. The MacDonald criteria did not account for changes in enhancement in response to certain drug use, like steroid and antiangiogenic agents, as well as post-treatment effects. The response is classified under the same headings as MacDonald’s criteria, with classification incorporating treatment-related inputs. These criteria assess enhancing lesions while also considering abnormalities in T2/FLAIR signaling. This approach aims to distinguish more accurately between genuine tumor response and conditions like pseudoprogression or pseudoresponse, especially in patients receiving concurrent temozolomide and antiangiogenic therapy.
Response Assessment in Pediatric Neuro-Oncology (RAPNO) (2020) [69]	<ul style="list-style-type: none"> The biology of high-grade gliomas differs significantly between children and adults, often necessitating distinct management approaches for pediatric patients. To address these differences, the Response Assessment in Pediatric Neuro-Oncology working group has recently issued guidelines for evaluating treatment responses in children with high-grade gliomas.
Brain Tumor—Reporting and Data System (BT-RADS) (2020) [70,71]	<ul style="list-style-type: none"> A structured reporting system to simplify and standardize MRI reporting of brain tumors. Provides guidance for imaging interpretation in follow-up post-treatment gliomas. The response is classified as BTRADS 0 (incomplete or no prior imaging), BTRADS 1 (improvement in imaging findings suggesting response), BTRADS 2 (stable imaging findings), BTRADS 3A (imaging findings suggestive of treatment-related worsening), BTRADS 3B (intermix of treatment-related worsening and disease-related worsening), BTRADS 3C (increase in disease burden), and BTRADS 4 (definitive increase in disease burden).

Table 4. Cont.

Criteria	Comment
	<ul style="list-style-type: none"> RANO 2.0 works on inputs from the original RANO criteria, modified RANO (mRANO) and immunotherapy RANO criteria (iRANO)
RANO 2.0 [72]	<ul style="list-style-type: none"> The groups remain as CR, PR, SD, and PD with additional inputs of treatment like radiotherapy and interval between therapy and imaging, use of steroids, and clinical deterioration and dissemination of disease in the form of leptomeningeal disease or non-measurable lesions.

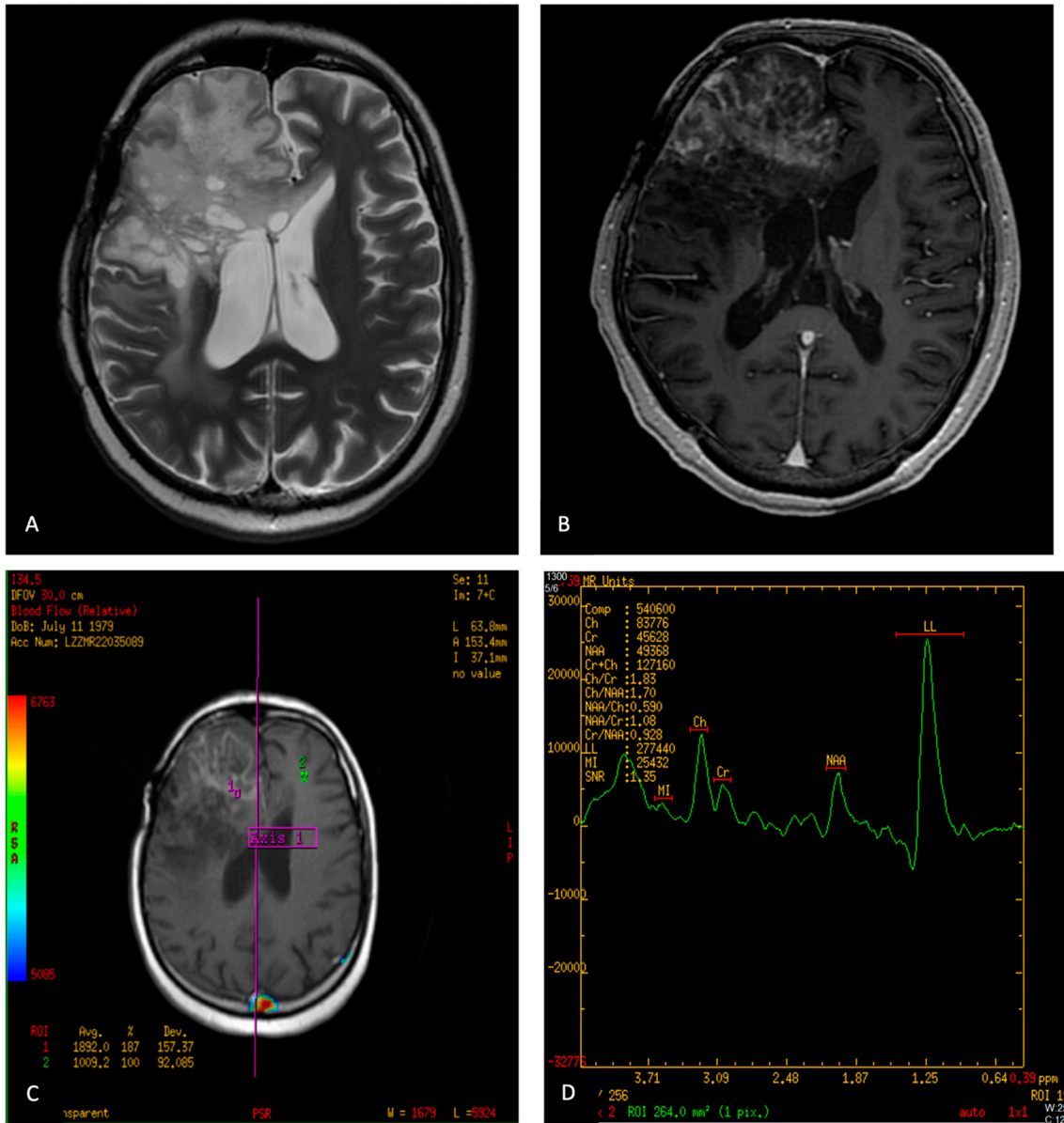


Figure 4. A 43-year-old male with anaplastic astrocytoma of right frontal glioma, post-EBRT with concurrent adjuvant temozolomide. Follow-up imaging 2 years after receiving radiation now demonstrates (A) Axial T2 W image with pericavitary hyperintensity in the right frontal-parietal region, extending along the rostrum of the corpus callosum. (B) Axial T1 W post-contrast image with an irregular feathery rim enhancing lesion (red arrow). (C) On MR perfusion, the corresponding areas show decreased rCBV. (D) On MR spectroscopy, elevated lipid/lactate peaks were confirmed with radiation necrosis.

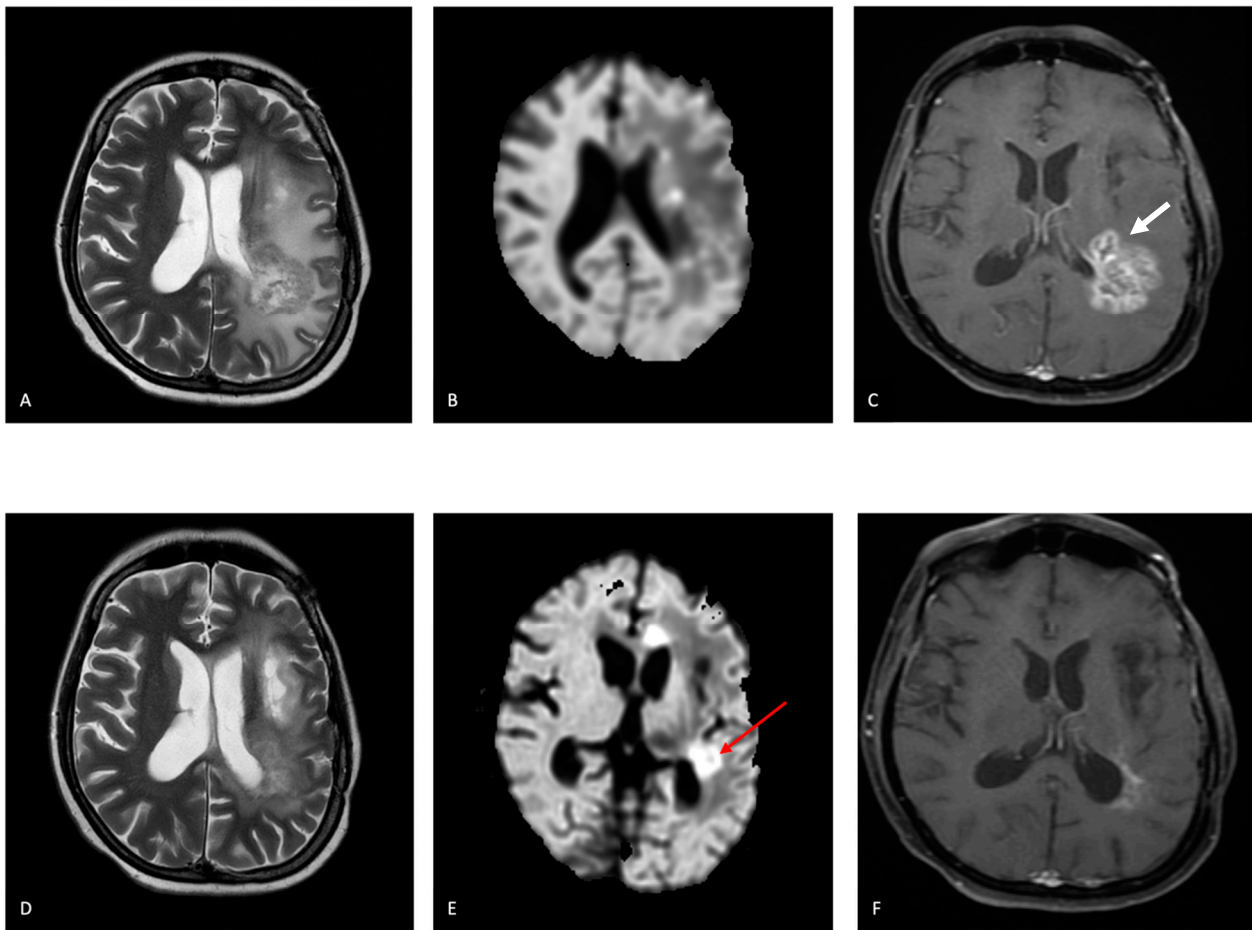


Figure 5. Tumor recurrence in a 47-year-old woman who underwent surgical resection and RT with temozolomide for infiltrating astrocytic tumor, IDH negative in the left parieto-insular region months earlier. (A) Axial T2-weighted image shows an intermediate lesion around the resection cavity. (B) The lesion is hypointense on a diffusion-weighted image. (C) Axial contrast-enhanced T1-weighted lesion with feathery enhancement consistent with recurrent disease (white arrow). Follow-up MR after 4 months post-two cycles of Bevacizumab. (D) Axial T2-weighted image shows a decrease in previously seen intermediate lesions. (E) The lesion (red arrow) shows restricted diffusion. (F) Axial contrast-enhanced T1-weighted lesion showing a decrease in the enhancing component suggestive of pseudoresponse.

5.5.2. Meningioma

Grade 1 meningiomas may be followed yearly for five years, followed by MRI every 2 years. For Grade 2 lesions, biannual follow-up is recommended for 5 years, followed by yearly intervals [46]. Grade 3 meningiomas, which are treated with maximally safe resection followed by radiotherapy, require closer follow-up intervals of 3–6 months. Resurgery or fractionated radiotherapy may be used in patients with recurrent meningiomas.

5.5.3. Pituitary Tumors

For incidental microadenomas, yearly MRI follow-up is recommended for the initial 3 years. If there is no increase in size after 3 years, the follow-up intervals may be prolonged.

For incidental macroadenomas, annual imaging follow-up is recommended. Visual field charting should be performed every 6 to 12 months.

For aggressive pituitary lesions, after completion of treatment, follow-up should occur every 3 to 12 months with imaging. The frequency of imaging depends on the rate of tumor growth and its proximity to important anatomical structures. Endocrine evaluation may be necessary based on the clinical scenario.

5.6. Role of Nuclear Medicine

Nuclear imaging can play an important role in differentiating CNS neoplasms from infections, primary from secondary tumors, and characterizing CNS primaries like lymphoma and glioma [73]. It also finds its utility in follow-up imaging in a few circumstances [74]. Applications of nuclear medicine in CNS tumor imaging are described in Table 5 [34,75–89].

Table 5. Role of nuclear imaging in CNS tumor imaging.

Modality	Tracers Available	Utility
Role of PET	<ul style="list-style-type: none"> • 18F-2-fluoro-2-deoxy-D-glucose (18F-FDG) • 11C-methyl-methionine (11C-MET) • O-(2-[18F]-fluoroethyl)-L-tyrosine (18F-FET) • 3,4-dihydroxy-6-[18F]-fluoro-L-phenylalanine (18F-FDOPA) • 68Ga-labeled tracers • DOTA-D-Phe1-Tyr3-octreotate (DOTATATE) • DOTA-Tyr3-octreotide (DOTATOC) • [18F]-GE-180-TSPO PET (Translocator protein) 	<p>Initial characterization—high SUV in lymphoma (FDG) Screening for primary (FDG) Glioma diagnosis and surveillance—in case of equivocal findings in MRI for treatment-related changes versus progression (FET-, F-DOPA) Somatostatin receptor analogs—specific for meningiomas (DOTATATE) TSPO-PET is a newer agent that is showing promising results in the diagnosis and follow-up of gliomas.</p>
Role of SPECT	<ul style="list-style-type: none"> • 99mTc-MIBI • 201Tl • 99mTc-DSMA • 99mTc-GHA • 99mTc-bismethionine-DTPA 	<p>Multiple studies in follow-up imaging of glioma show variable sensitivity and specificity of these techniques (80–95%) as compared with DSC-PWI and MRS.</p>

6. Role of Artificial Intelligence in Primary CNS Neoplasms

The applications of Artificial Intelligence in diagnosis, planning of management, post-treatment follow-up, and outcome prediction have been widely studied in gliomas [90].

6.1. Pre-Treatment Prediction

Pre-treatment prediction of histology, along with other features like tumor grade in glioma, IDH mutation status, EGFR amplification, and MGMT promoter methylation, have been extensively studied, and various AI-based models have been developed in this field [91–97]. The process entails segmentation by separating tumor tissue from healthy parenchyma, initially by a radiologist, followed by the use of this segmented region of interest to identify specific radiomic features with quantifiable measurements. However, due to the high interobserver variability of manual segmentation, automatic segmentation methods have been devised to increase accuracy and save human time. The Brain Tumor Segmentation Challenge (BraTS) is an annual challenge where the organizing committee releases large volumes of multimodal scans of many patients with glioma in an open forum for research groups to construct machine learning (ML) algorithms to facilitate the automatic segmentation process. These data are accompanied by corresponding segmentation that can serve as the ground truth for the process [98] (Figure 6).

6.2. Pseudoprogression

Pseudoprogression (PP) is a treatment-associated condition in primary and secondary brain neoplasms, but it has been best described in relation to gliomas, presenting early during treatment and associated with imaging with or without clinical worsening. Advanced imaging techniques like PWI are generally employed to differentiate PP from true progression (TP). However, as PWI is dependent on technique, post-processing, and interpretation, AI methods have been tried to solve this diagnostic dilemma [99]. A study by Lao et al. has shown that a deep learning-based radiomics model using multiparametric imaging that included conventional MRI, DWI, and PWI for differentiating PP from TP in 61 glioblastoma patients within 3 months after radio-chemotherapy and surgical resection performed better than any single parameter by the LASSO logistic regression model, with

an AUC = 0.90 [99]. Another study performed on 78 glioma patients showed an AUC = 0.83 to differentiate PP from TP using the hybrid deep and machine learning CNN-LSTM (long short-term memory) method. The dataset comprised clinical features and imaging findings extracted from post-contrast MRI. These models should be tested in multi-institutional settings to validate their clinical utility.

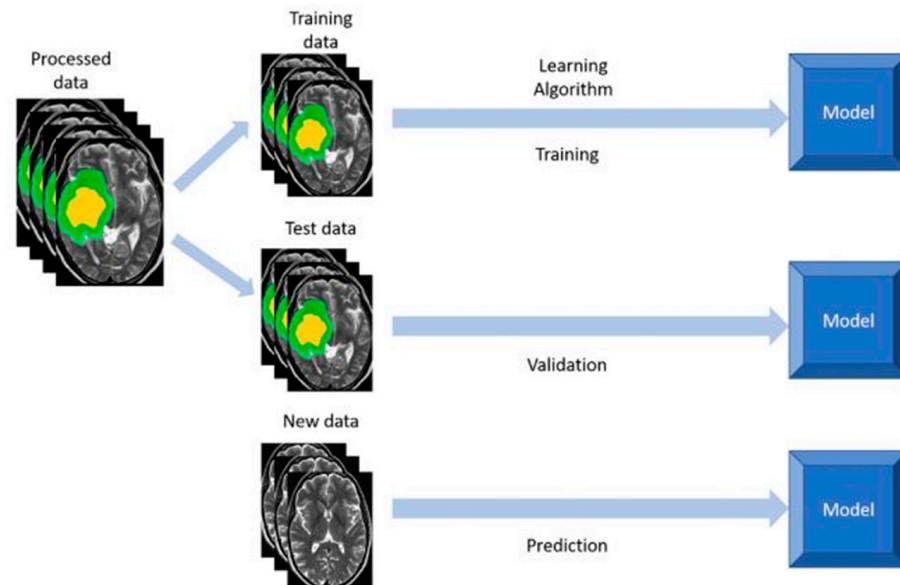


Figure 6. Schematic diagram demonstrates an artificial intelligence algorithm where the machine is trained using training data. Algorithm is validated using validation data. After validation, test data are given for prediction.

6.3. Radiation Necrosis (RN) and True Progression/Recurrence (Treatment Response Evaluation)

In a study conducted by Zhang et al., both handcrafted and deep features were integrated from multimodality MRI scans. They developed logistic regression models aimed at distinguishing glioma recurrence from radiation necrosis. The top-performing model achieved exceptional metrics in the validation phase, including an Area Under the Curve (AUC) of 0.99, sensitivity of 0.99, and specificity of 0.97. This advanced model demonstrated enhanced capability in characterizing tumor heterogeneity, effectively predicting either glioma recurrence or radiation necrosis with high accuracy [94]. A combined approach of quantitative radiomics features from MRI, clinical features, and MGMT promoter methylation status can complement each other for the development of better-performing models for the prediction of treatment response in glioblastoma [100,101]. A systematic review of 18 studies on machine learning applications in evaluating treatment response in glioblastoma found that ML models using MRI features showed promising diagnostic performance in distinguishing progression from mimics. However, concerns were raised regarding the quality and design of the studies [102]. Another meta-analysis of 9 studies aimed at distinguishing true progression from pseudoprogression reported a sensitivity of 95.2% (95% CI: 86.6–98.4%) and specificity of 82.4% (95% CI: 67.0–91.6%). Nevertheless, similar limitations were noted. Despite the promising outlook of AI and ML in monitoring treatment response in glioma, these technologies are still in their early stages and require external validation and larger datasets to mitigate overfitting before their clinical utility can be fully realized [103].

6.4. Role of AI in Imaging of Other Primary CNS Neoplasms

A host of studies have investigated the role of machine learning techniques in differentiating different tumor types [104]. Kim et al. differentiated glioblastoma (GBM) from primary CNS lymphoma (PCNSL) using multiparametric MRI-based radiomics with an AUC of 0.95 [105]. Another study differentiated between the two based on texture

features on multiparametric MRI and showed that rCBV offered the highest AUC of 0.86 for distinguishing GBM from PCNSL [106]. A study by Niu et al. to differentiate between different subtypes of meningioma using basic MRI-based radiomics demonstrated accuracies between 98.8% and 100% [107]. Dong et al. differentiated pilocytic astrocytoma from GBM by a decision tree model with a validation set accuracy of 86% [108]. Another study by Zhang et al. used MRI-based radiomics to differentiate between non-functioning pituitary adenoma subtypes with contrast T1 weighted images showing AUC of 0.83 and 0.80 in training and test sets, respectively [109]. Multiple other studies have been performed to differentiate between different tumors with AUCs ranging from 0.81 to 0.97 [110,111].

7. Summary

Malignant primary CNS neoplasms are a significant cause of morbidity and mortality in the adult population. MRI imaging forms the cornerstone for guiding the diagnosis, treatment, and follow-up of intracranial neoplasms. Multiparametric MRI can help guide biopsy and surgery and serves as a problem-solving tool in cases posing diagnostic dilemmas during post-treatment follow-up. Various diagnostic criteria have been developed to guide post-treatment response evaluation. Nuclear medicine acts as an adjunct in challenging situations, such as post-treatment evaluation of gliomas to rule out progression versus pseudoprogression/radiation necrosis and differentiating meningiomas from other dura-based lesions like metastasis. Artificial intelligence finds numerous applications in brain tumor imaging and can aid in designing faster workflows. However, future studies should benefit from external validation and larger datasets to reduce overfitting and increase accuracy.

Author Contributions: Conceptualization, A.M.; methodology, A.M. and K.B.; resources, A.M. and K.B.; data curation, K.B.; writing—original draft preparation, K.B.; writing—review and editing, A.M. and K.B.; visualization, A.M. and K.B.; supervision, A.M.; project administration, K.B. All authors have read and agreed to the published version of the manuscript.

Funding: This research received no external funding.

Conflicts of Interest: The authors declare no conflicts of interest.

References

1. Ostrom, Q.T.; Price, M.; Neff, C.; Cioffi, G.; Waite, K.A.; Kruchko, C.; Barnholtz-Sloan, J.S. CBTRUS Statistical Report: Primary Brain and Other Central Nervous System Tumors Diagnosed in the United States in 2015–2019. *Neuro-Oncol.* **2022**, *24* (Suppl. S5), v1–v95. [[CrossRef](#)]
2. Dasgupta, A.; Gupta, T.; Jalali, R. Indian data on central nervous tumors: A summary of published work. *South Asian J. Cancer* **2016**, *5*, 147–153. [[CrossRef](#)] [[PubMed](#)]
3. Osborn, A.G. *Osborn's Brain: Imaging, Pathology and Anatomy*, 2nd ed.; Elsevier: Amsterdam, The Netherlands, 2017.
4. Alomar, S.A. Clinical manifestation of central nervous system tumor. *Semin. Diagn. Pathol.* **2010**, *27*, 97–104. [[CrossRef](#)] [[PubMed](#)]
5. Ferreira, M.P.; Ferreira, N.P.; Filho, A.A.P.; Filho, G.A.P.; Franciscatto, A.C. Stereotactic computed tomography-guided brain biopsy: Diagnostic yield based on a series of 170 patients. *Surg. Neurol.* **2006**, *65*, S27–S32. [[CrossRef](#)] [[PubMed](#)]
6. Patnaik, S.; Jyotsnarani, Y.; Uppin, S.G.; Susarla, R. Imaging features of primary tumors of the spine: A pictorial essay. *Indian J. Radiol. Imaging* **2016**, *26*, 279–289. [[CrossRef](#)] [[PubMed](#)] [[PubMed Central](#)]
7. Bhattacharya, K.; Rastogi, S.; Mahajan, A. Post-treatment imaging of gliomas: Challenging the existing dogmas. *Clin. Radiol.* **2024**, *79*, e376–e392. [[CrossRef](#)] [[PubMed](#)]
8. Aydın, Z.B.; Aydın, H.; Birgi, E.; Hekimoğlu, B. Diagnostic Value of Diffusion-weighted Magnetic Resonance (MR) Imaging, MR Perfusion, and MR Spectroscopy in Addition to Conventional MR Imaging in Intracranial Space-occupying Lesions. *Cureus* **2019**, *11*, e6409. [[CrossRef](#)] [[PubMed](#)]
9. Wang, Q.; Zhang, J.; Xu, W.; Chen, X.; Zhang, J.; Xu, B. Role of magnetic resonance spectroscopy to differentiate high-grade gliomas from metastases. *Tumor Biol.* **2017**, *39*, 1010428317710030. [[CrossRef](#)]
10. Neska-Matuszewska, M.; Bladowska, J.; Sasiadek, M.; Zimny, A. Differentiation of glioblastoma multiforme, metastases and primary central nervous system lymphomas using multiparametric perfusion and diffusion MR imaging of a tumor core and a peritumoral zone-Searching for a practical approach. *PLoS ONE* **2018**, *13*, e0191341. [[CrossRef](#)]
11. Seo, M.; Choi, Y.; Soo Lee, Y.; Ahn, K.-J.; Kim, B.-S.; Park, J.-S.; Jeon, S.S. Glioma grading using multiparametric MRI: Head-to-head comparison among dynamic susceptibility contrast, dynamic contrast-enhancement, diffusion-weighted images, and MR spectroscopy. *Eur. J. Radiol.* **2023**, *165*, 110888. [[CrossRef](#)]

12. Kong, L.-W.; Chen, J.; Zhao, H.; Yao, K.; Fang, S.-Y.; Wang, Z.; Wang, Y.-Y.; Li, S.-W. Intratumoral Susceptibility Signals Reflect Biomarker Status in Gliomas. *Sci. Rep.* **2019**, *9*, 17080. [[CrossRef](#)]
13. Manan, A.A.; Yahya, N.; Idris, Z.; Manan, H.A. The Utilization of Diffusion Tensor Imaging as an Image-Guided Tool in Brain Tumor Resection Surgery: A Systematic Review. *Cancers* **2022**, *14*, 2466. [[CrossRef](#)] [[PubMed](#)]
14. Nadkarni, T.N.; Andreoli, M.J.; Nair, V.A.; Yin, P.; Young, B.M.; Kundu, B.; Pankratz, J.; Radtke, A.; Holdsworth, R.; Kuo, J.S.; et al. Usage of fMRI for pre-surgical planning in brain tumor and vascular lesion patients: Task and statistical threshold effects on language lateralization. *NeuroImage Clin.* **2015**, *7*, 415–423. [[CrossRef](#)] [[PubMed](#)]
15. Asao, C.; Korogi, Y.; Kitajima, M.; Hirai, T.; Baba, Y.; Makino, K.; Kochi, M.; Morishita, S.; Yamashita, Y. Diffusion-weighted imaging of radiation-induced brain injury for differentiation from tumor recurrence. *AJNR Am. J. Neuroradiol.* **2005**, *26*, 1455–1460. [[PubMed](#)]
16. Hein, P.A.; Eskey, C.J.; Dunn, J.F.; Hug, E.B. Diffusion-weighted imaging in the follow-up of treated high-grade gliomas: Tumor recurrence versus radiation injury. *AJNR Am. J. Neuroradiol.* **2004**, *25*, 201–209. [[PubMed](#)]
17. van Dijken, B.R.J.; van Laar, P.J.; Holtman, G.A.; van der Hoorn, A. Diagnostic accuracy of magnetic resonance imaging techniques for treatment response evaluation in patients with high-grade glioma, a systematic review and meta-analysis. *Eur. Radiol.* **2017**, *27*, 4129–4144. [[CrossRef](#)]
18. Zhang, H.; Ma, L.; Wang, Q.; Zheng, X.; Wu, C.; Xu, B.-N. Role of magnetic resonance spectroscopy for the differentiation of recurrent glioma from radiation necrosis: A systematic review and meta-analysis. *Eur. J. Radiol.* **2014**, *83*, 2181–2189. [[CrossRef](#)]
19. Barajas, R.F., Jr.; Chang, J.S.; Segal, M.R.; Parsa, A.T.; McDermott, M.W.; Berger, M.S.; Cha, S. Differentiation of recurrent glioblastoma multiforme from radiation necrosis after external beam radiation therapy with dynamic susceptibility-weighted contrast-enhanced perfusion MR imaging. *Radiology* **2009**, *253*, 486–496. [[CrossRef](#)]
20. Clarke, J.L.; Chang, S. Pseudoprogression and pseudoresponse: Challenges in brain tumor imaging. *Curr. Neurol. Neurosci. Rep.* **2009**, *9*, 241–246. [[CrossRef](#)]
21. Nguyen, H.S.; Milbach, N.; Hurrell, S.L.; Cochran, E.; Connelly, J.; Bovi, J.A.; Schultz, C.J.; Mueller, W.M.; Rand, S.D.; Schmainda, K.M.; et al. Progressing Bevacizumab-Induced Diffusion Restriction Is Associated with Coagulative Necrosis Surrounded by Viable Tumor and Decreased Overall Survival in Patients with Recurrent Glioblastoma. *AJNR Am. J. Neuroradiol.* **2016**, *37*, 2201–2208. [[CrossRef](#)]
22. Chung, J.Y.; Lee, J.J.; Kim, H.J.; Seo, H.Y. Characterization of Magnetic Resonance Images for Spinal Cord Tumors. *Asian Spine J.* **2008**, *2*, 15–21. [[CrossRef](#)]
23. Yuh, E.L.; Barkovich, A.J.; Gupta, N. Imaging of ependymomas: MRI and CT. *Childs Nerv. Syst.* **2009**, *25*, 1203–1213. [[CrossRef](#)] [[PubMed](#)]
24. Tang, M.Y.; Chen, T.W.; Zhang, X.M.; Huang, X.H. GRE T2*-weighted MRI: Principles and clinical applications. *BioMed Res. Int.* **2014**, *2014*, 312142. [[CrossRef](#)] [[PubMed](#)]
25. Allam, K.E.; Elkhalek, Y.I.A.; Hassan, H.G.E.M.A.; Emara, M.A.E. Diffusion-weighted magnetic resonance imaging in differentiation between different vertebral lesions using ADC mapping as a quantitative assessment tool. *Egypt. J. Radiol. Nucl. Med.* **2022**, *53*, 155. [[CrossRef](#)]
26. Ahmad, F.U.; Li, D.C.; Malcolm, J.G.; Rindler, R.S.; Baum, G.R.; Rao, A.; Khurpad, S.N. The role of diffusion tensor imaging in spinal pathology: A review. *Neurol. India* **2017**, *65*, 982–992. [[CrossRef](#)] [[PubMed](#)]
27. Li, Z.; Chen, Y.A.; Chow, D.; Talbott, J.; Glastonbury, C.; Shah, V. Practical applications of CISS MRI in spine imaging. *Eur. J. Radiol. Open* **2019**, *6*, 231–242. [[CrossRef](#)]
28. Shi, J.; Zhang, Y.; Yao, B.; Sun, P.; Hao, Y.; Piao, H.; Zhao, X. Application of Multiparametric Intraoperative Ultrasound in Glioma Surgery. *BioMed Res. Int.* **2021**, *2021*, 6651726. [[CrossRef](#)]
29. Moiyadi, A.V.; Kannan, S.; Shetty, P. Navigated intraoperative ultrasound for resection of gliomas: Predictive value, influence on resection and survival. *Neurol. India* **2015**, *63*, 727–735. [[CrossRef](#)]
30. Neugut, A.I.; Sackstein, P.; Hillyer, G.C.; Jacobson, J.S.; Bruce, J.; Lassman, A.B.; Stieg, P.A. Magnetic Resonance Imaging-Based Screening for Asymptomatic Brain Tumors: A Review. *Oncologist* **2018**, *24*, 375–384. [[CrossRef](#)]
31. Prada, C.E.; Hufnagel, R.B.; Hummel, T.R.; Lovell, A.M.; Hopkin, R.J.; Saal, H.M.; Schorry, E.K. The Use of Magnetic Resonance Imaging Screening for Optic Pathway Gliomas in Children with Neurofibromatosis Type. *J. Pediatr.* **2015**, *167*, 851–856.e1. [[CrossRef](#)]
32. Consul, N.; Amini, B.; Ibarra-Rovira, J.J.; Blair, K.J.; Moseley, T.W.; Taher, A.; Shah, K.B.; Elsayes, K.M. Li-Fraumeni Syndrome and Whole-Body MRI Screening: Screening Guidelines, Imaging Features, and Impact on Patient Management. *Am. J. Roentgenol.* **2021**, *216*, 252–263. [[CrossRef](#)]
33. Daly, M.B.; Pal, T.; Berry, M.P.; Buys, S.S.; Dickson, P.; Domchek, S.M.; Elkhanany, A.; Friedman, S.; Goggins, M.; Hutton, M.L.; et al. Genetic/Familial High-Risk Assessment: Breast, Ovarian, and Pancreatic, Version 2.2021, NCCN Clinical Practice Guidelines in Oncology. *J. Natl. Compr. Cancer Netw. JNCCN* **2021**, *19*, 77–102. [[CrossRef](#)] [[PubMed](#)]
34. Engelhard, H.H.; Corsten, L.A. Leptomeningeal Metastasis of Primary Central Nervous System (CNS) Neoplasms. In *Leptomeningeal Metastases*; Abrey, L.E., Chamberlain, M.C., Engelhard, H.H., Eds.; Springer: Boston, MA, USA, 2005; pp. 71–85.
35. Tiefenbach, J.; Lu, V.M.; Metzler, A.R.; Palejwala, A.; Haider, S.; Ivan, M.E.; Komotar, R.J.; Shah, A.H. The use of advanced neuroimaging modalities in the evaluation of low-grade glioma in adults: A literature review. *Neurosurg. Focus* **2024**, *56*, E3. [[CrossRef](#)] [[PubMed](#)]

36. Hasan, A.-M.S.; Megally, H.I.; Khallaf, M.; Haseib, A. The combined role of MR spectroscopy and perfusion imaging in preoperative differentiation between high- and low-grade gliomas. *Egypt. J. Radiol. Nucl. Med.* **2019**, *50*, 72. [[CrossRef](#)]
37. Villanueva-Meyer, J.E.; Mabray, M.C.; Cha, S. Current Clinical Brain Tumor Imaging. *Neurosurgery* **2017**, *81*, 397–415. [[CrossRef](#)]
38. Al-Okaili, R.N.; Krejza, J.; Woo, J.H.; Wolf, R.L.; O'Rourke, D.M.; Judy, K.D.; Poptani, H.; Melhem, E.R. Intraaxial Brain Masses: MR Imaging-based Diagnostic Strategy—Initial Experience. *Radiology* **2007**, *243*, 539–550. [[CrossRef](#)]
39. Singhal, V. Clinical Approach to Acute Decline in Sensorium. *Indian J. Crit. Care Med.* **2019**, *23* (Suppl. S2), S120–S123.
40. Maschio, M.; Aguglia, U.; Avanzini, G.; Banfi, P.; Buttinelli, C.; Capovilla, G.; Luisa Casazza, M.M.; Colicchio, G.; Coppola, A.; Costa, C.; et al. Management of epilepsy in brain tumors. *Neurol. Sci.* **2019**, *40*, 2217–2234. [[CrossRef](#)] [[PubMed](#)]
41. Dietrich, J.; Rao, K.; Pastorino, S.; Kesari, S. Corticosteroids in brain cancer patients: Benefits and pitfalls. *Expert Rev. Clin. Pharmacol.* **2011**, *4*, 233–242. [[CrossRef](#)]
42. Weller, M.; van den Bent, M.; Preusser, M.; Le Rhun, E.; Tonn, J.C.; Minniti, G.; Bendszus, M.; Balana, C.; Chinot, O.; Dirven, L.; et al. EANO guidelines on the diagnosis and treatment of diffuse gliomas of adulthood. *Nat. Rev. Clin. Oncol.* **2021**, *18*, 170–186. [[CrossRef](#)]
43. Akshulakov, S.K.; Kerimbayev, T.T.; Biryuchkov, M.Y.; Urunbayev, Y.A.; Farhadi, D.S.; Byvaltsev, V.A. Current Trends for Improving Safety of Stereotactic Brain Biopsies: Advanced Optical Methods for Vessel Avoidance and Tumor Detection. *Front. Oncol.* **2019**, *9*, 947. [[CrossRef](#)]
44. Zhao, Z.; Zhang, K.-N.; Wang, Q.; Li, G.; Zeng, F.; Zhang, Y.; Wu, F.; Chai, R.; Wang, Z.; Zhang, C.; et al. Chinese Glioma Genome Atlas (CGGA): A Comprehensive Resource with Functional Genomic Data from Chinese Glioma Patients. *Genom. Proteom. Bioinform.* **2021**, *19*, 1–12. [[CrossRef](#)] [[PubMed](#)]
45. McFaline-Figueroa, J.R.; Lee, E.Q. Brain Tumors. *Am. J. Med.* **2018**, *131*, 874–882. [[CrossRef](#)] [[PubMed](#)]
46. Goldbrunner, R.; Stavrinou, P.; Jenkinson, M.D.; Sahm, F.; Mawrin, C.; Weber, D.C.; Preusser, M.; Minniti, G.; Lund-Johansen, M.; Lefranc, F.; et al. EANO guideline on the diagnosis and management of meningiomas. *Neuro-Oncol.* **2021**, *23*, 1821–1834. [[CrossRef](#)] [[PubMed](#)]
47. Molitch, M.E. Diagnosis and Treatment of Pituitary Adenomas: A Review. *JAMA* **2017**, *317*, 516–524. [[CrossRef](#)]
48. von Baumgarten, L.; Illerhaus, G.; Korfel, A.; Schlegel, U.; Deckert, M.; Dreyling, M. The Diagnosis and Treatment of Primary CNS Lymphoma. *Dtsch. Arztebl. Int.* **2018**, *115*, 419–426. [[CrossRef](#)]
49. Hoang-Xuan, K.; Deckert, M.; Ferreri, A.J.M.; Furtner, J.; Perez-Larraya, J.G.; Henriksson, R.; Hottinger, A.F.; Kasenda, B.; Lefranc, F.; Lossos, A.; et al. European Association of Neuro-Oncology (EANO) guidelines for treatment of primary central nervous system lymphoma (PCNSL). *Neuro-Oncol.* **2023**, *25*, 37–53. [[CrossRef](#)]
50. Kamepalli, H.; Kalaparti, V.; Kesavadas, C. Imaging Recommendations for the Diagnosis, Staging, and Management of Adult Brain Tumors. *Indian J. Med. Paediatr. Oncol.* **2023**, *44*, 026–038. [[CrossRef](#)]
51. Riche, M.; Amelot, A.; Peyre, M.; Capelle, L.; Carpentier, A.; Mathon, B. Complications after frame-based stereotactic brain biopsy: A systematic review. *Neurosurg. Rev.* **2021**, *44*, 301–307. [[CrossRef](#)] [[PubMed](#)]
52. Shetty, P.; Yeole, U.; Singh, V.; Moiyadi, A. Navigated ultrasound-based image guidance during resection of gliomas: Practical utility in intraoperative decision-making and outcomes. *Neurosurg. Focus* **2021**, *50*, E14. [[CrossRef](#)]
53. Moiyadi, A.V.; Shetty, P.; John, R. Non-enhancing gliomas: Does intraoperative ultrasonography improve resections? *Ultrasonography* **2019**, *38*, 156–165. [[CrossRef](#)]
54. Hu, X.; Xu, R.; Ding, H.; Lv, R.; Yang, L.; Wang, Y.; Xie, R. The total resection rate of glioma can be improved by the application of US-MRI fusion combined with contrast-enhanced ultrasound. *Clin. Neurol. Neurosurg.* **2021**, *208*, 106892. [[CrossRef](#)] [[PubMed](#)]
55. Bush, N.A.O.; Chang, S.M.; Berger, M.S. Current and future strategies for treatment of glioma. *Neurosurg. Rev.* **2017**, *40*, 1–14. [[CrossRef](#)] [[PubMed](#)]
56. Huang, R.Y.; Bi, W.L.; Griffith, B.; Kaufmann, T.J.; la Fougère, C.; Schmidt, N.O.; Tonn, J.C.; A Vogelbaum, M.; Wen, P.Y.; Aldape, K.; et al. Imaging and diagnostic advances for intracranial meningiomas. *Neuro-Oncol.* **2019**, *21*, i44–i61. [[CrossRef](#)] [[PubMed](#)]
57. Walker, A.J.; Ruzevick, J.; Malayeri, A.A.; Rigamonti, D.; Lim, M.; Redmond, K.J.; Kleinberg, L. Postradiation imaging changes in the CNS: How can we differentiate between treatment effect and disease progression? *Future Oncol.* **2014**, *10*, 1277–1297. [[CrossRef](#)] [[PubMed](#)]
58. Brandsma, D.; Stalpers, L.; Taal, W.; Sminia, P.; van den Bent, M.J. Clinical features, mechanisms, and management of pseudoprogression in malignant gliomas. *Lancet Oncol.* **2008**, *9*, 453–461. [[CrossRef](#)] [[PubMed](#)]
59. Rane, N.; Quaghebeur, G. CNS effects following the treatment of malignancy. *Clin. Radiol.* **2012**, *67*, 61–68. [[CrossRef](#)]
60. Ellingson, B.M.; Chung, C.; Pope, W.B.; Boxerman, J.L.; Kaufmann, T.J. Pseudoprogression, radionecrosis, inflammation or true tumor progression? challenges associated with glioblastoma response assessment in an evolving therapeutic landscape. *J. Neuro-Oncol.* **2017**, *134*, 495–504. [[CrossRef](#)]
61. Wang, Y.X.; King, A.D.; Zhou, H.; Leung, S.F.; Abrigo, J.; Chan, Y.L.; Hu, C.W.; Yeung, D.K.W.; Ahuja, A.T. Evolution of radiation-induced brain injury: MR imaging-based study. *Radiology* **2010**, *254*, 210–218. [[CrossRef](#)]
62. Shah, R.; Vattoth, S.; Jacob, R.; Manzil, F.F.P.; O'malley, J.P.; Borghei, P.; Patel, B.N.; Curé, J.K. Radiation necrosis in the brain: Imaging features and differentiation from tumor recurrence. *RadioGraphics* **2012**, *32*, 1343–1359. [[CrossRef](#)]
63. Mullins, M.E.; Barest, G.D.; Schaefer, P.W.; Hochberg, F.H.; Gonzalez, R.G.; Lev, M. Radiation necrosis versus glioma recurrence: Conventional MR imaging clues to diagnosis. *AJNR Am. J. Neuroradiol.* **2005**, *26*, 1967–1972.

64. Kazda, T.; Bulik, M.; Pospisil, P.; Lakomy, R.; Smrcka, M.; Slampa, P.; Jancalek, R. Advanced MRI increases the diagnostic accuracy of recurrent glioblastoma: Single institution thresholds and validation of MR spectroscopy and diffusion weighted MR imaging. *NeuroImage Clin.* **2016**, *11*, 316–321. [[CrossRef](#)] [[PubMed](#)]
65. Bernstock, J.D.; E Gary, S.; Klinger, N.; A Valdes, P.; Ibn Essayed, W.; E Olsen, H.; Chagoya, G.; Elsayed, G.; Yamashita, D.; Schuss, P.; et al. Standard clinical approaches and emerging modalities for glioblastoma imaging. *Neuro-Oncol. Adv.* **2022**, *4*, v000080. [[CrossRef](#)] [[PubMed](#)]
66. Boothe, D.; Young, R.; Yamada, Y.; Prager, A.; Chan, T.; Beal, K. Bevacizumab as a treatment for radiation necrosis of brain metastases post stereotactic radiosurgery. *Neuro-Oncol.* **2013**, *15*, 1257–1263. [[CrossRef](#)] [[PubMed](#)]
67. Macdonald, D.R.; Cascino, T.L.; Schold, S.C.; Cairncross, J.G., Jr. Response criteria for phase II studies of supratentorial malignant glioma. *J. Clin. Oncol.* **1990**, *8*, 1277–1280. [[CrossRef](#)] [[PubMed](#)]
68. Wen, P.Y.; Macdonald, D.R.; Reardon, D.A.; Cloughesy, T.F.; Sorensen, A.G.; Galanis, E.; DeGroot, J.; Wick, W.; Gilbert, M.R.; Lassman, A.B.; et al. Updated response assessment criteria for high-grade gliomas: Response assessment in neuro-oncology working group. *J. Clin. Oncol.* **2010**, *28*, 1963–1972. [[CrossRef](#)]
69. Erker, C.; Tamrazi, B.; Poussaint, T.Y.; Mueller, S.; Mata-Mbemba, D.; Franceschi, E.; A Brandes, A.; Rao, A.; Haworth, K.B.; Wen, P.Y.; et al. Response assessment in paediatric high-grade glioma: Recommendations from the Response Assessment in Pediatric Neuro-Oncology (RAPNO) working group. *Lancet Oncol.* **2020**, *21*, e317–e329. [[CrossRef](#)]
70. Zhang, J.Y.; Weinberg, B.D.; Hu, R.; Saindane, A.; Mullins, M.; Allen, J.; Hoch, M.J. Quantitative Improvement in Brain Tumor MRI Through Structured Reporting (BT-RADS). *Acad. Radiol.* **2020**, *27*, 780–784. [[CrossRef](#)]
71. Kim, S.; Hoch, M.J.; Peng, L.; Somasundaram, A.; Chen, Z.; Weinberg, B.D. A brain tumor reporting and data system to optimize imaging surveillance and prognostication in high-grade gliomas. *J. Neuroimaging* **2022**, *32*, 1185–1192. [[CrossRef](#)] [[PubMed](#)]
72. Wen, P.Y.; Bent, M.V.D.; Youssef, G.; Cloughesy, T.F.; Ellingson, B.M.; Weller, M.; Galanis, E.; Barboriak, D.P.; de Groot, J.; Gilbert, M.R.; et al. RANO 2.0: Update to the Response Assessment in Neuro-Oncology Criteria for High- and Low-Grade Gliomas in Adults. *J. Clin. Oncol.* **2023**, *41*, 5187–5199. [[CrossRef](#)] [[PubMed](#)] [[PubMed Central](#)]
73. Raverot, G.; Burman, P.; McCormack, A.; Heaney, A.; Petersenn, S.; Popovic, V.; Trouillas, J.; Dekkers, O.M.; European Society of Endocrinology. European Society of Endocrinology Clinical Practice Guidelines for the management of aggressive pituitary tumours and carcinomas. *Eur. J. Endocrinol.* **2018**, *178*, G1–G24. [[CrossRef](#)]
74. Galldiks, N.; Niyazi, M.; Grosu, A.L.; Kocher, M.; Langen, K.-J.; Law, I.; Minniti, G.; Kim, M.M.; Tsien, C.; Dhermain, F.; et al. Contribution of PET imaging to radiotherapy planning and monitoring in glioma patients—A report of the PET/RANO group. *Neuro-Oncol.* **2021**, *23*, 881–893. [[CrossRef](#)] [[PubMed](#)]
75. Verger, A.; Kas, A.; Darcourt, J.; Guedj, E. PET Imaging in Neuro-Oncology: An Update and Overview of a Rapidly Growing Area. *Cancers* **2022**, *14*, 1103. [[CrossRef](#)] [[PubMed](#)]
76. Fink, J.R.; Muzi, M.; Peck, M.; Krohn, K.A. Multimodality Brain Tumor Imaging: MR Imaging, PET, and PET/MR Imaging. *J. Nucl. Med.* **2015**, *56*, 1554–1561. [[CrossRef](#)] [[PubMed](#)]
77. Treglia, G.; Muoio, B.; Trevisi, G.; Mattoli, M.V.; Albano, D.; Bertagna, F.; Giovanella, L. Diagnostic Performance and Prognostic Value of PET/CT with Different Tracers for Brain Tumors: A Systematic Review of Published Meta-Analyses. *Int. J. Mol. Sci.* **2019**, *20*, 4669. [[CrossRef](#)] [[PubMed](#)]
78. Galldiks, N.; Lohmann, P.; Albert, N.L.; Tonn, J.C.; Langen, K.-J. Current status of PET imaging in neuro-oncology. *Neuro-Oncol. Adv.* **2019**, *1*, v00010. [[CrossRef](#)]
79. Lewington, V.; Hughes, S.J. Nuclear medicine functional imaging of the brain. *Clin. Med.* **2012**, *12*, 364–368. [[CrossRef](#)]
80. Giovacchini, G.; Riondato, M.; Giovannini, E.; Ciarmiello, A. Diagnostic Applications of Nuclear Medicine: Brain Tumors. In *Nuclear Oncology: From Pathophysiology to Clinical Applications*; Strauss, H.W., Mariani, G., Volterrani, D., Larson, S.M., Eds.; Springer International Publishing: Cham, Switzerland, 2017; pp. 467–505.
81. Zhang, J.; Traylor, K.S.; Mountz, J.M. PET and SPECT Imaging of Brain Tumors. *Semin. Ultrasound CT MRI* **2020**, *41*, 530–540. [[CrossRef](#)]
82. Shooli, H.; Dadgar, H.; Wang, Y.-X.J.; Vafae, M.S.; Kashuk, S.R.; Nemati, R.; Jafari, E.; Nabipour, I.; Gholamrezanezhad, A.; Assadi, M.; et al. An update on PET-based molecular imaging in neuro-oncology: Challenges and implementation for a precision medicine approach in cancer care. *Quant. Imaging Med. Surg.* **2019**, *9*, 1597–1610. [[CrossRef](#)]
83. Valotassiou, V.; Leondi, A.; Angelidis, G.; Psimadas, D.; Georgoulas, P. SPECT and PET imaging of meningiomas. *Sci. World J.* **2012**, *2012*, 412580. [[CrossRef](#)]
84. Al-Faham, Z.; Kassir, M.A.; Wood, D.; Balon, H.R. Appearance of Meningioma on ^{99m}Tc-HMPAO SPECT: Correlation with MRI. *J. Nucl. Med. Technol.* **2016**, *44*, 90–91. [[CrossRef](#)]
85. Jeune, F.P.; Dubois, F.; Blond, S.; Steinling, M. Sestamibi technetium-99m brain single-photon emission computed tomography to identify recurrent glioma in adults: 201 studies. *J. Neuro-Oncol.* **2006**, *77*, 177–183. [[CrossRef](#)] [[PubMed](#)]
86. Tie, J.; Gunawardana, D.H.; Rosenthal, M.A. Differentiation of tumor recurrence from radiation necrosis in high-grade gliomas using 201Tl-SPECT. *J. Clin. Neurosci.* **2008**, *15*, 1327–1334. [[CrossRef](#)] [[PubMed](#)]
87. Santra, A.; Sharma, P.; Kumar, R.; Bal, C.; Kumar, A.; Julka, P.K.; Malhotra, A. Comparison of glucoheptonate single photon emission computed tomography and contrast-enhanced MRI in detection of recurrent glioma. *Nucl. Med. Commun.* **2011**, *32*, 206–211. [[CrossRef](#)]

88. Rani, N.; Singh, B.; Kumar, N.; Singh, P.; Hazari, P.P.; Singh, H. Differentiation of Recurrent/Residual Glioma From Radiation Necrosis Using Semi Quantitative ^{99m}Tc MDM (Bis-Methionine-DTPA) Brain SPECT/CT and Dynamic Susceptibility Contrast-Enhanced MR Perfusion: A Comparative Study. *Clin. Nucl. Med.* **2018**, *43*, e74–e81. [[CrossRef](#)] [[PubMed](#)]
89. Filippi, L.; Frantellizzi, V.; De Vincentis, G.; Schillaci, O.; Evangelista, L. Clinical Applications of TSPO PET for Glioma Imaging: Current Evidence and Future Perspective—A Systematic Review. *Diagnostics* **2023**, *13*, 1813. [[CrossRef](#)] [[PubMed](#)] [[PubMed Central](#)]
90. Li, D.; Patel, C.B.; Xu, G.; Iagaru, A.; Zhu, Z.; Zhang, L.; Cheng, Z. Visualization of Diagnostic and Therapeutic Targets in Glioma With Molecular Imaging. *Front. Immunol.* **2020**, *11*, 592389. [[CrossRef](#)]
91. Mahajan, A.; Sahu, A.; Ashtekar, R.; Kulkarni, T.; Shukla, S.; Agarwal, U.; Bhattacharya, K. Glioma radiogenomics and artificial intelligence: Road to precision cancer medicine. *Clin. Radiol.* **2022**, *78*, 137–149. [[CrossRef](#)]
92. Davatzikos, C.; Barnholtz-Sloan, J.S.; Bakas, S.; Colen, R.; Mahajan, A.; Quintero, C.B.; Font, J.C.; Puig, J.; Jain, R.; E Sloan, A.; et al. AI-based prognostic imaging biomarkers for precision neuro-oncology: The ReSPOND consortium. *Neuro-Oncol.* **2020**, *22*, 886–888. [[CrossRef](#)]
93. Zhang, Q.; Cao, J.; Zhang, J.; Bu, J.; Yu, Y.; Tan, Y.; Feng, Q.; Huang, M. Differentiation of Recurrence from Radiation Necrosis in Gliomas Based on the Radiomics of Combinational Features and Multimodality MRI Images. *Comput. Math. Methods Med.* **2019**, *2019*, 2893043. [[CrossRef](#)]
94. Choy, G.; Khalilzadeh, O.; Michalski, M.; Synho, D.; Samir, A.E.; Pinykh, O.S.; Geis, J.R.; Pandharipande, P.V.; Brink, J.A.; Dreyer, K.J. Current Applications and Future Impact of Machine Learning in Radiology. *Radiology* **2018**, *288*, 318–328. [[CrossRef](#)]
95. Drabycz, S.; Roldán, G.; de Robles, P.; Adler, D.; McIntyre, J.B.; Magliocco, A.M.; Cairncross, J.G.; Mitchell, J.R. An analysis of image texture, tumor location, and MGMT promoter methylation in glioblastoma using magnetic resonance imaging. *NeuroImage* **2010**, *49*, 1398–1405. [[CrossRef](#)] [[PubMed](#)]
96. Chen, S.; Xu, Y.; Ye, M.; Li, Y.; Sun, Y.; Liang, J.; Lu, J.; Wang, Z.; Zhu, Z.; Zhang, X.; et al. Predicting MGMT Promoter Methylation in Diffuse Gliomas Using Deep Learning with Radiomics. *J. Clin. Med.* **2022**, *11*, 3445. [[CrossRef](#)] [[PubMed](#)]
97. Bakas, S.; Akbari, H.; Pisapia, J.; Martinez-Lage, M.; Rozycki, M.; Rathore, S.; Davatzikos, C. In Vivo Detection of EGFRvIII in Glioblastoma via Perfusion Magnetic Resonance Imaging Signature Consistent with Deep Peritumoral Infiltration: The ϕ -Index. *Clin. Cancer Res.* **2017**, *23*, 4724–4734. [[CrossRef](#)]
98. van Kempen, E.J.; Post, M.; Mannil, M.; Witkam, R.L.; ter Laan, M.; Patel, A.; Meijer, F.J.A.; Henssen, D. Performance of machine learning algorithms for glioma segmentation of brain MRI: A systematic literature review and meta-analysis. *Eur. Radiol.* **2021**, *31*, 9638–9653. [[CrossRef](#)]
99. Lao, J.; Chen, Y.; Li, Z.C.; Li, Q.; Zhang, J.; Liu, J.; Zhai, G. A Deep Learning-Based Radiomics Model for Prediction of Survival in Glioblastoma Multiforme. *Sci. Rep.* **2017**, *7*, 10353. [[CrossRef](#)]
100. Zhou, Q.; Xue, C.; Ke, X.; Zhou, J. Treatment Response and Prognosis Evaluation in High-Grade Glioma: An Imaging Review Based on MRI. *J. Magn. Reson. Imaging* **2022**, *56*, 325–340. [[CrossRef](#)]
101. Booth, T.C.; Grzeda, M.; Chelliah, A.; Roman, A.; Al Busaidi, A.; Dragos, C.; Shuaib, H.; Luis, A.; Mirchandani, A.; Alparlan, B.; et al. Imaging Biomarkers of Glioblastoma Treatment Response: A Systematic Review and Meta-Analysis of Recent Machine Learning Studies. *Front. Oncol.* **2022**, *12*, 799662. [[CrossRef](#)]
102. Bhandari, A.; Marwah, R.; Smith, J.; Nguyen, D.; Bhatti, A.; Lim, C.P.; Lasocki, A. Machine learning imaging applications in the differentiation of true tumour progression from treatment-related effects in brain tumours: A systematic review and meta-analysis. *J. Med. Imaging Radiat. Oncol.* **2022**, *66*, 781–797. [[CrossRef](#)] [[PubMed](#)]
103. Henriksen, O.M.; Álvarez-Torres, M.d.M.; Figueiredo, P.; Hangel, G.; Keil, V.C.; Nechifor, R.E.; Riemer, F.; Schmainda, K.M.; Warnert, E.A.H.; Wieggers, E.C.; et al. High-Grade Glioma Treatment Response Monitoring Biomarkers: A Position Statement on the Evidence Supporting the Use of Advanced MRI Techniques in the Clinic, and the Latest Bench-to-Bedside Developments. Part 1: Perfusion and Diffusion Techniques. *Front. Oncol.* **2022**, *12*, 810263. [[CrossRef](#)]
104. Afridi, M.; Jain, A.; Aboian, M.; Payabvash, S. Brain Tumor Imaging: Applications of Artificial Intelligence. *Semin. Ultrasound CT MRI* **2022**, *43*, 153–169. [[CrossRef](#)] [[PubMed](#)]
105. Kim, Y.; Cho, H.-H.; Kim, S.T.; Park, H.; Nam, D.; Kong, D.-S. Radiomics features to distinguish glioblastoma from primary central nervous system lymphoma on multi-parametric MRI. *Neuroradiology* **2018**, *60*, 1297–1305. [[CrossRef](#)] [[PubMed](#)]
106. Nakagawa, M.; Nakaura, T.; Namimoto, T.; Kitajima, M.; Uetani, H.; Tateishi, M.; Oda, S.; Utsunomiya, D.; Makino, K.; Nakamura, H.; et al. Machine learning based on multi-parametric magnetic resonance imaging to differentiate glioblastoma multiforme from primary cerebral nervous system lymphoma. *Eur. J. Radiol.* **2018**, *108*, 147–154. [[CrossRef](#)] [[PubMed](#)]
107. Niu, L.; Zhou, X.; Duan, C.; Zhao, J.; Sui, Q.; Liu, X.; Zhang, X.J.Z. Differentiation Researches on the Meningioma Subtypes by Radiomics from Contrast-Enhanced Magnetic Resonance Imaging: A Preliminary Study. *World Neurosurg.* **2019**, *126*, e646–e652. [[CrossRef](#)] [[PubMed](#)]
108. Dong, F.; Li, Q.; Xu, D.; Xiu, W.; Zeng, Q.; Zhu, X.; Xu, F.; Jiang, B.; Zhang, M. Differentiation between pilocytic astrocytoma and glioblastoma: A decision tree model using contrast-enhanced magnetic resonance imaging-derived quantitative radiomic features. *Eur. Radiol.* **2019**, *29*, 3968–3975. [[CrossRef](#)] [[PubMed](#)]
109. Zhang, S.; Song, G.; Zang, Y.; Jia, J.; Wang, C.; Li, C.; Tian, J.; Dong, D.; Zhang, Y. Non-invasive radiomics approach potentially predicts non-functioning pituitary adenomas subtypes before surgery. *Eur. Radiol.* **2018**, *28*, 3692–3701. [[CrossRef](#)] [[PubMed](#)]

110. Shrot, S.; Salhov, M.; Dvorski, N.; Konen, E.; Averbuch, A.; Hoffmann, C. Application of MR morphologic, diffusion tensor, and perfusion imaging in the classification of brain tumors using machine learning scheme. *Neuroradiology* **2019**, *61*, 757–765. [[CrossRef](#)] [[PubMed](#)]
111. Chakrabarty, S.; Sotiras, A.; Milchenko, M.; LaMontagne, P.; Hileman, M.; Marcus, D. MRI-based Identification and Classification of Major Intracranial Tumor Types by Using a 3D Convolutional Neural Network: A Retrospective Multi-institutional Analysis. *Radiol. Artif. Intell.* **2021**, *3*, e200301. [[CrossRef](#)] [[PubMed](#)] [[PubMed Central](#)]

Disclaimer/Publisher’s Note: The statements, opinions and data contained in all publications are solely those of the individual author(s) and contributor(s) and not of MDPI and/or the editor(s). MDPI and/or the editor(s) disclaim responsibility for any injury to people or property resulting from any ideas, methods, instructions or products referred to in the content.